Advances in Science and Technology Research Journal

Advances in Science and Technology Research Journal, 2026, 20(6), 488–510
https://doi.org/10.12913/22998624/218127
ISSN 2299-8624, License CC-BY 4.0

Received: 2026.01.06
Accepted: 2026.04.15
Published: 2026.05.01

Designating the unmanned aerial vehicle kinematic position using weighted mean model for integration of corrections from EGNOS, UK SBAS, and AL-SBAS augmentation systems

Kamil Krasuski[1*], Damian Wierzbicki[2]

[1] Faculty of Navigation and Logistic, Polish Air Force University, ul. Dywizjonu 303 nr 35, 08-521 Dęblin, Poland
[2] Faculty of Civil Engineering and Geodesy, Military University of Technology, ul. Gen. S. Kaliskiego 2, 00-908 Warsaw 46, Poland
* Corresponding author's e-mail: k.krasuski@law.mil.pl

ABSTRACT

The primary objective of this paper is to develop an algorithm for integrating a user's kinematic position solution based on corrections provided by the EGNOS, UK SBAS, and AL-SBAS systems. To date, aviation research in Poland has primarily employed a single EGNOS augmentation system. In contrast, this study is the first to use three independent satellite-based augmentation systems (SBAS) within a single experiment, which constitutes a novelty in this research area. This approach is crucial for ensuring redundancy in position determination and for controlling the calculations of the determined coordinates. To this end, a weighted mean model was applied to determine the user's coordinates. Measurement weights were defined as functions of the inverse number of tracked satellites and the inverse of the point position error ellipsoid. Using the proposed computational strategy, the user position was determined in ellipsoidal coordinates (BLh), and the precision of the solution was additionally assessed by calculating the standard deviation and the mean error of the arithmetic mean. The computational strategy was validated through an airborne experiment using a VTOL WingtraOne UAV equipped with a NovAtel OEM7500 GNSS receiver. The results indicate that the mean value of the standard deviation of the determined position does not exceed 3.01 m when measurement weights are defined as the inverse of the number of tracked satellites, and 2.60 m when weights are defined as the inverse of the point position error ellipsoid. Weighting observations using the inverse of the point position error ellipsoid produced better results, as it is calculated based on the actual mean measurement errors. The proposed research methodology can be applied to other SBAS augmentation systems within areas of overlapping correction coverage. In particular, the developed methodology can be applied to SBAS APV approach-to-landing operations in air navigation.

Keywords: satellite-based augmentation system, EGNOS, UK SBAS, AL-SBAS, unmanned aerial vehicle, ellipsoidal coordinates.

INTRODUCTION

Since 2003, research activities in Poland have focused on the application of Satellite-Based Augmentation Systems (SBAS) in air transportation [1, 2]. The first SBAS implemented in aviation navigation was the European Geostationary Navigation Overlay Service (EGNOS) [3], which remains officially certified for aviation applications in Poland to this day [4]. Over more than two decades of operational use, EGNOS has continuously supported and enhanced kinematic GPS positioning performance in air transport across this part of Europe [5]. However, according to the International GNSS Service (IGS) [6], the global constellation of SBAS augmentation systems has been steadily expanding, resulting in an increasing number of geostationary satellites providing correction signals over extensive regions of the Earth [7]. Due to Poland's geographical location, its territory lies within the coverage areas of several SBAS systems, including the

European EGNOS, the United Kingdom SBAS (UK SBAS), and the Algerian AL-SBAS. While the correction coverage of EGNOS and UK SBAS extends over the entire country, the coverage of AL-SBAS is limited to latitudes up to 50°N. Consequently, all three SBAS systems can be utilized for aviation operations in southern Poland. From an operational perspective, the coexistence of multiple SBAS systems over a relatively limited geographical area may pose certain challenges. From a scientific standpoint, however, this situation is highly advantageous, as it enables comprehensive airborne research on multiple SBAS systems under comparable conditions. Of particular importance is the determination of user position coordinates based on correction data from EGNOS [8], UK SBAS [9], and AL-SBAS [10]. Among all GNSS navigation data, the accurate estimation of user position is a fundamental task. This aspect becomes even more critical in kinematic scenarios, such as airborne experiments, where precise and reliable position determination is essential for navigation performance assessment. Therefore, the integration of correction data from multiple SBAS systems represents a promising approach to improving the reliability and robustness of kinematic positioning solutions. By combining independent SBAS-based navigation solutions, it is possible to enhance redundancy in position determination, thereby increasing confidence in the obtained results for individual measurement epochs. Such a strategy is particularly relevant for improving flight safety in aviation navigation, as well as for supporting emerging applications involving unmanned aerial vehicles (UAVs).

Multi-SBAS studies in which more than one SBAS system was used in Poland can be found, among others, in publications [11–13]. The studies determined both the precision and the accuracy of aircraft coordinates during flight tests. The research methodology was based on a weighted mean model and an arithmetic mean model. In the case of the weighted mean model, the weighting coefficients were defined as a function of the inverse of the number of tracked GPS satellites and as a function of the inverse of the geometric dilution of precision (DOP) factor. In the arithmetic mean model, the measurement weights were equal to 1. The studies used corrections from the EGNOS and SDCM augmentation systems. The background to the described studies [11–13] is the fact that only a single EGNOS system is currently used in aviation operations [1–4]. This results in reliance on single coordinate readings, a lack of quality control of SBAS corrections, no comparison of the estimated GNSS receiver coordinates, and no redundancy of navigation position solutions. Consequently, Multi-SBAS solutions are far superior, as they enable the fusion and integration of SBAS data. In Multi-SBAS positioning, at least two SBAS augmentation systems are considered, as already described in publications [11–13]. However, Multi-SBAS positioning may also involve the use of three SBAS systems, which is the focus of the present study. This is particularly interesting as it also concerns the UK SBAS and AL-SBAS augmentation systems, which have not been used in aviation operations in Poland. Moreover, it should be emphasized that during SBAS data fusion, various weighting strategies can be applied within the position integration model. Therefore, it is not necessary to rely solely on the measurement weights presented in publications [11–13], as they may be determined using a different algorithm. The concept of the research project presented in this paper involves conducting a UAV flight during which GPS and SBAS data from the EGNOS, UK SBAS, and AL-SBAS augmentation systems will be collected. Subsequently, a GNSS data fusion and integration model in the form of a weighted mean model will be developed. This will make it possible to determine the user's position in the form of geodetic coordinates BLh, as well as additional precision measures in the form of the standard deviation and the mean error of the arithmetic mean. The overall research concept is illustrated in Figure 1.

BACKGROUND

As stated in the introduction, this study focuses on three SBAS augmentation systems, namely EGNOS, UK SBAS and AL-SBAS [14]. It is therefore necessary to review the most important scientific publications and research achievements related to the aviation application of these SBAS systems. Table 1 shows the main research achievements based on EGNOS, UK SBAS, and AL-SBAS support systems. Most of the completed studies concerned the EGNOS augmentation system, primarily focusing on aviation navigation flight tests. All GNSS positioning quality parameters in aviation were examined, i.e. accuracy, continuity, availability, and integrity.

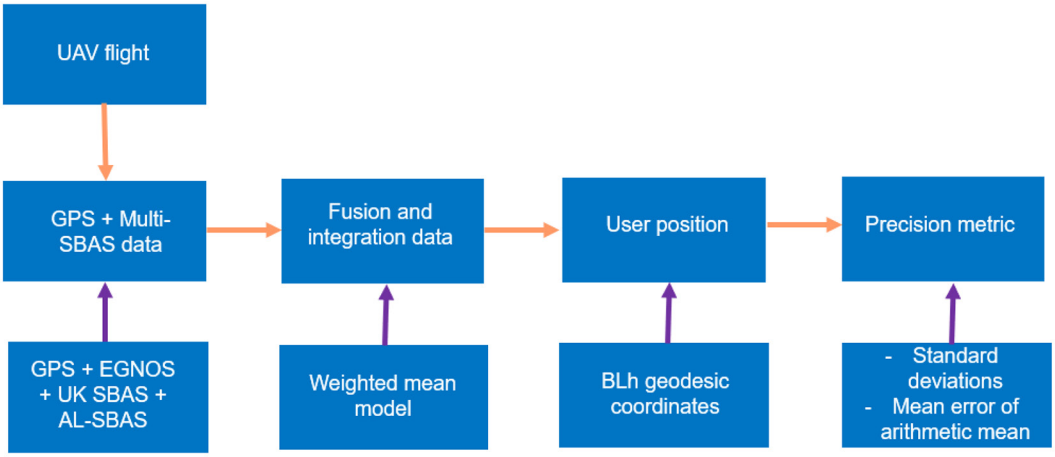

Figure 1. The overall concept of research in paper

In addition, EGNOS was used to monitor atmospheric changes as part of modeling ionospheric and tropospheric corrections. A considerable number of studies were devoted to EGNOS signal analysis, the application of EGNOS in landing approach procedures, and the monitoring of PBN navigation performance. A separate issue involves application trends in the use of EGNOS in UAV technology. Research on the UK SBAS system mainly concerns the determination of GNSS positioning quality parameters in aviation and the analysis of the SBAS signal in the context of landing approach procedures. In the case of the AL-SBAS system, studies also address the determination of GNSS positioning quality parameters in aviation and atmospheric monitoring, primarily of the ionosphere. Based on the conducted analysis of the state of the knowledge, the following key conclusions can be drawn:

- the majority of aviation research in Poland and worldwide has been conducted using the EGNOS augmentation system;
- only limited aviation studies have been performed worldwide using the UK SBAS and AL-SBAS systems;
- applications of UK SBAS in air transportation have been reported in Poland;
- no studies concerning aviation applications of AL-SBAS have been published in Poland;
- aviation studies involving EGNOS, UK SBAS and AL-SBAS have been conducted separately for each system, without attempts to integrate SBAS corrections;

Table 1. Characteristic of the main research achievements based on EGNOS, UK SBAS, and AL-SBAS support systems

Tested parameter	Selected publications	SBAS systems used	Conclusions for further research
GNSS positioning quality parameters in aviation	[1, 3, 5, 8, 14–27, 37, 39, 40, 42, 43, 58]	EGNOS, UK SBAS, AL-SBAS	All studies reported in the literature have been conducted separately for the EGNOS, UK SBAS, and AL-SBAS systems. There is a clear need to perform flight experiments using all three SBAS systems simultaneously. This need is particularly evident in the context of Poland, where the majority of studies have focused exclusively on EGNOS, while research on UK SBAS is limited to a single publication [58], and no studies addressing the AL-SBAS system have been reported to date. Consequently, it is necessary to develop a dedicated methodology, mathematical algorithms, and data fusion strategies for integrating corrections from the three SBAS augmentation systems in order to improve user positioning performance.
Monitoring atmospheric parameters	[28-30, 38, 50, 51]	EGNOS, AL-SBAS	
SBAS signal analysis in approach procedures, including the development of PBN navigation performance	[9, 31–36, 41, 44–49]	EGNOS, UK SBAS	
SBAS applications for UAV technology	[52–57]	EGNOS	

- research has addressed both manned aircraft and UAV platforms;
- existing studies have primarily focused on positioning quality assessment and SBAS signal monitoring in approach-to-landing procedures.

RESEARCH PROBLEM

This section defines the research problems identified on the basis of the conducted analysis of the state of the knowledge. As demonstrated in the previous section, the simultaneous application of three SBAS augmentation systems—EGNOS, UK SBAS, and AL-SBAS—in kinematic user positioning is a particularly relevant issue for aviation navigation within the transportation domain. Such an approach is highly beneficial in aviation navigation, as it introduces redundancy in the determination of user position coordinates. Consequently, the user gains the ability to verify the obtained positioning results at individual measurement epochs, which is a critical aspect of navigation reliability. From the perspective of flight safety, the proposed concept of integrating multiple SBAS-based positioning solutions is of significant importance. The availability of independent position estimates derived from different SBAS systems allows for increased robustness of the navigation solution, particularly in dynamic, kinematic scenarios such as airborne experiments and UAV operations.

The most important research problems identified in the context of this study can be summarized as follows:

- Is it possible to simultaneously apply EGNOS, UK SBAS, and AL-SBAS corrections within a single flight test for user position determination?
- If so, what mathematical model should be adopted to describe user position estimation based on EGNOS, UK SBAS, and AL-SBAS corrections?
- How should EGNOS, UK SBAS, and AL-SBAS data be integrated within a navigation positioning solution?
- What computational methodology and processing strategy should be adopted to support such an integration?

The success criteria for the development of an algorithm integrating EGNOS, UK SBAS, and AL-SBAS data primarily include:

- acquisition, procurement, and operational use of a GNSS receiver capable of tracking and recording SBAS corrections from the EGNOS, UK SBAS, and AL-SBAS systems in kinematic tests;
- recording GPS and Multi-SBAS data with a defined time interval (e.g. 1 s);
- synchronization of Multi-SBAS data across all measurement epochs;
- verification of the consistency of the Multi-SBAS navigation data sets, ensuring that the number of observations is identical for all three SBAS systems;
- importing GPS and Multi-SBAS data stored in text files into a selected numerical programming environment;
- development of a complete numerical script in accordance with the assumed research methodology and computational strategy;
- final execution of the numerical script and validation of its functionality with respect to the implemented mathematical algorithms.

Addressing these research gaps is essential for advancing SBAS-based kinematic positioning in aviation navigation. The development of an integrated SBAS positioning model has the potential to improve the precision and accuracy of navigation solutions for both manned and unmanned aerial platforms operating in regions with overlapping SBAS correction coverage. Naturally, improvements in precision and accuracy are not achievable without prior modification of the mathematical algorithm describing the method for determining the user's kinematic coordinates. Therefore, the primary objective of this study is to specify the mathematical algorithm for user position determination, which will ultimately enable the computation of precision and accuracy parameters.

MATERIALS AND METHODS

The adopted research methodology was divided into three main stages. First, an airborne experiment was performed using a VTOL WingtraOne unmanned aerial vehicle (UAV). A NovAtel OEM7500 GNSS receiver installed on the UAV platform recorded GPS observations and navigation messages, as well as SBAS corrections from the EGNOS, UK SBAS and AL-SBAS systems in real time during the flight. GPS observations,

expressed as pseudorange measurements, were recorded at a 1 s interval, similarly to the SBAS corrections. GPS observations and navigation messages were stored in the RINEX format [59], while SBAS corrections were saved in the EMS format [60]. During the experiment, EGNOS corrections transmitted by satellite S123, UK SBAS corrections from satellite S158 and AL-SBAS corrections from satellite S148 were used. The collected GPS/SBAS data enabled the computation of three independent navigation solutions, namely GPS/EGNOS, GPS/UK SBAS and GPS/AL-SBAS. Thus, the UAV position could be determined in three different ways. This provided the basis for developing a position integration model based on a weighted mean approach using measurement weights. In this study, two weighting strategies taken from the literature were adopted. In the first case, weighting is calculated as a function of the inverse number of tracked satellites [41]. In this way, the weight of the measurement depends on the geometry of the GPS satellites. In strategy no. 2 the weight is defined as a function of the inverse of the point position error ellipsoid [2]. In this way, the measurement weight depends on the mean errors of user coordinates from a single GPS/SBAS solution. Using these strategies, a resultant UAV position together with its precision was determined. The UAV position was expressed in ellipsoidal coordinates BLh according the ICAO recommendations [1]. The precision was evaluated in the form of the standard deviation and the mean error of the arithmetic mean. In addition, the accuracy parameter was estimated also as a position errors. Results of accuracy will be presented in Chapter of discussion. The precision and accuracy parameters were also expressed in the BLh ellipsoidal coordinate frame [4]. This has a direct impact on the units of precision and accuracy, which are expressed in meters. The full flowchart was presented into Figure 2.

After a brief description of the research methodology, the mathematical algorithms applied in this study are introduced. Once the GNSS data from the UAV flight were collected, individual GPS/SBAS navigation solutions—GPS/EGNOS, GPS/UK SBAS and GPS/AL-SBAS—were first computed. These calculations were performed using RTKLIB v.2.4.3 software [61]. RTKLIB applies the Single Point Positioning (SPP) code-based positioning method with SBAS corrections in the navigation solution [62]. As a result, three independent UAV coordinate solutions were obtained from GPS/EGNOS, GPS/UK SBAS and GPS/AL-SBAS positioning. The next step involved the development of an integration model for combining the individual GPS/SBAS position solutions. The general form of the weighted mean model is expressed by Equation 1:

$$\begin{cases} B_w = \frac{\sum_{i=1}^{n} B_i \cdot P_{i,j}}{\sum_{i=1}^{n} P_{i,j}} \\ L_w = \frac{\sum_{i=1}^{n} L_i \cdot P_{i,j}}{\sum_{i=1}^{n} P_{i,j}} \\ h_w = \frac{\sum_{i=1}^{n} h_i \cdot P_{i,j}}{\sum_{i=1}^{n} P_{i,j}} \end{cases} \quad (1)$$

where: B_W – the resultant value of Latitude obtained from the weighted mean model, L_W – the resultant value of longitude obtained from the weighted mean model,

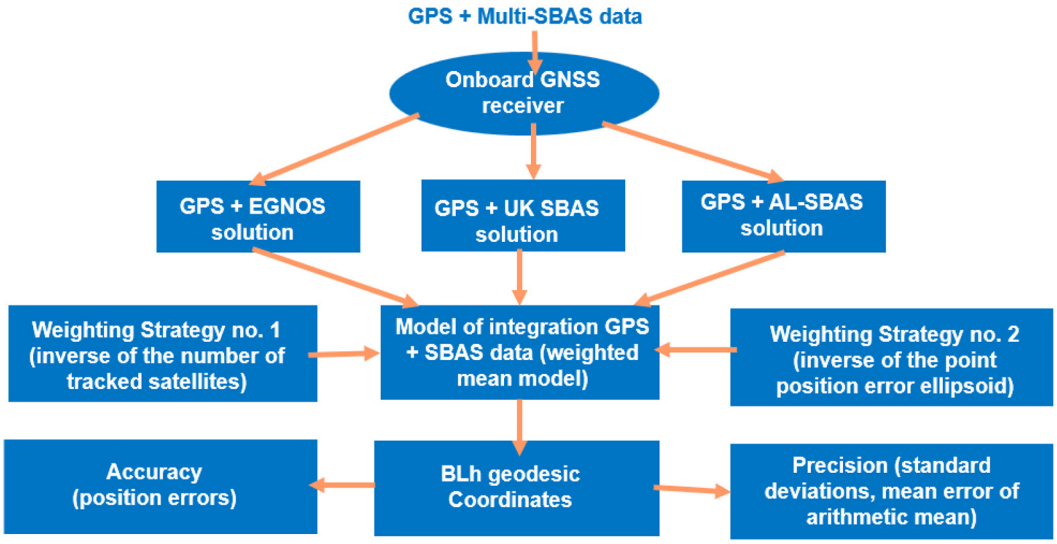

Figure 2. The flowchart of research method

h_W – the resultant value of ellipsoidal height obtained from the weighted mean model, B_i – the individual value of latitude obtained from the GPS/EGNOS, or GPS/UK SBAS or GPS/AL-SBAS solution, L_i – the individual value of Longitude obtained from the GPS/EGNOS, or GPS/UK SBAS or GPS/AL-SBAS solution, h_i – the individual value of ellipsoidal height obtained from the GPS/EGNOS, or GPS/UK SBAS or GPS/AL-SBAS solution, i – the index denoting a given GPS/EGNOS or GPS/UK SBAS or GPS/AL-SBAS, i = (1: GPS/EGNOS, 2: GPS/UK SBAS, 3: GPS/AL – SBAS), n – the total number of individual GPS/SBAS position solutions GPS/SBAS, n = 3, $P_{i,j}$ – the measurement weight corresponding to a given GPS/SBAS solution and computational strategy, j – the index denoting the computational strategy, j = (1: strategy no. 1, 2: strategy no. 2).

Equation 1 combines individual GPS/SBAS solutions to determine the resultant UAV position expressed in ellipsoidal coordinates BLh. The resultant position is determined with a number of degrees of freedom defined by Equation 2 [63]:

$$f = n - 1 = 2 \tag{2}$$

where: f – number of degrees of freedom.

In a detailed form, the proposed Equation 1 will take two forms:

- for strategy no. 1:

$$\begin{cases} B_w = \frac{B_1 \cdot P_{1,1} + B_2 \cdot P_{2,1} + B_3 \cdot P_{3,1}}{P_{1,1} + P_{2,1} + P_{3,1}} \\ L_w = \frac{L_1 \cdot P_{1,1} + L_2 \cdot P_{2,1} + L_3 \cdot P_{3,1}}{P_{1,1} + P_{2,1} + P_{3,1}} \\ h_w = \frac{h_1 \cdot P_{1,1} + h_2 \cdot P_{2,1} + h_3 \cdot P_{3,1}}{P_{1,1} + P_{2,1} + P_{3,1}} \end{cases} \tag{3}$$

- or for strategy no. 2:

$$\begin{cases} B_w = \frac{B_1 \cdot P_{1,2} + B_2 \cdot P_{2,2} + B_3 \cdot P_{3,2}}{P_{1,2} + P_{2,2} + P_{3,2}} \\ L_w = \frac{L_1 \cdot P_{1,2} + L_2 \cdot P_{2,2} + L_3 \cdot P_{3,2}}{P_{1,2} + P_{2,2} + P_{3,2}} \\ h_w = \frac{h_1 \cdot P_{1,2} + h_2 \cdot P_{2,2} + h_3 \cdot P_{3,2}}{P_{1,2} + P_{2,2} + P_{3,2}} \end{cases} \tag{4}$$

where: B_1 – single value of Latitude from GPS/EGNOS solution, L_1 – single value of Longitude from GPS/EGNOS solution, h_1 – single value of ellipsoidal height from GPS/EGNOS solution, B_2 – single value of Latitude from GPS/UK SBAS solution, L_2 – single value of Longitude from GPS/UK SBAS solution, h_2 – single value of ellipsoidal height from GPS/UK SBAS solution, B_3 – single value of Latitude from GPS/ AL-SBAS solution, L_3 – single value of Longitude from GPS/AL-SBAS solution, h_3 – single value of ellipsoidal height from GPS/AL-SBAS solution, $P_{1,1}$ – measuring scale from the GPS/EGNOS solution for calculation strategy no. 1, $P_{1,2}$ – measuring scale from the GPS/EGNOS solution for calculation strategy no. 2, $P_{2,1}$ – measurement weight from the GPS/UK SBAS solution for calculation strategy no. 1, $P_{2,2}$ – measurement weight from the GPS/UK SBAS solution for calculation strategy no. 2, $P_{3,1}$ – measuring scale from the GPS/AL-SBAS solution for calculation strategy no. 1, $P_{3,2}$ – measuring scale from the GPS/AL-SBAS solution for calculation strategy no. 2.

In algorithm (3–4), different models of measurement weights were proposed according to strategies no. 1 and 2. In strategy no. 1, the measurement weights were calculated as the inverse of the number of tracked satellites [2, 41, 56] in the form:

$$\begin{cases} P_{1,1} = \frac{1}{NS_1} \\ P_{2,1} = \frac{1}{NS_2} \\ P_{3,1} = \frac{1}{NS_3} \end{cases} \tag{5}$$

where: NS_1 – number of satellites in the GPS/EGNOS solution, NS_2 – number of satellites in the GPS/UK SBAS solution, NS_3 – number of satellites in the GPS/AL-SBAS solution.

In strategy no. 2, the measurement weights were calculated as the inverse of the point position error ellipsoid [64, 65] in the form:

$$\begin{cases} P_{1,2} = \frac{1}{CL_1} \\ P_{2,2} = \frac{1}{CL_2} \\ P_{3,2} = \frac{1}{CL_3} \end{cases} \tag{6}$$

where: CL_1 – ellipsoid of the point position error in the GPS/EGNOS solution, $CL_1 = \sqrt{mB_1^2 + mL_1^2 + mh_1^2}$, mB_1 – mean error of Latitude from GPS/EGNOS solution [42, 66, 67], mL_1 – mean error of Longitude from GPS/EGNOS solution

[42, 66, 67], mh_1 – mean error of ellipsoidal height from GPS/EGNOS solution [42, 66, 67], CL_2 – point position error ellipsoid in the GPS/UK SBAS solution, $CL_2 = \sqrt{mB_2^2 + mL_2^2 + mh_2^2}$, mB_2 – mean error of Latitude from GPS/UK SBAS solution [42, 66, 67], mL_2 – mean error of Longitude from GPS/UK SBAS solution [42, 66, 67], mh_2 – mean error of ellipsoidal height from GPS/UK SBAS solution [42, 66, 67], CL_3 – ellipsoid of the point position error in the GPS/AL-SBAS solution, $CL_3 = \sqrt{mB_3^2 + mL_3^2 + mh_3^2}$, mB_3 – mean error of Latitude from GPS/AL-SBAS solution [42, 66, 67], mL_3 – mean error of Longitude from GPS/AL-SBAS solution [42, 66, 67], mh_3 – mean error of ellipsoidal height from GPS/AL-SBAS solution [42, 66, 67].

The presented algorithm (1–6) is implemented in parallel for computational strategies 1 and 2. Therefore, the resultant coordinates of the UAV's position will be calculated in two ways. The quality of the determined UAV position coordinates will be determined primarily by specific statistical precision parameters, i.e., standard deviations and mean error of the arithmetic mean. The standard deviation is described [56, 68, 69] for BLh coordinates as below:

- for strategy no. 1:

$$\begin{cases} StdB_w = \sqrt{\frac{VB_1^T \cdot P_{1,1} \cdot VB_1 + VB_2^T \cdot P_{2,1} \cdot VB_2 + VB_3^T \cdot P_{3,1} \cdot VB_3}{f}} \\ StdL_w = \sqrt{\frac{VL_1^T \cdot P_{1,1} \cdot VL_1 + VL_2^T \cdot P_{2,1} \cdot VL_2 + VL_3^T \cdot P_{3,1} \cdot VL_3}{f}} \\ Stdh_w = \sqrt{\frac{Vh_1^T \cdot P_{1,1} \cdot Vh_1 + Vh_2^T \cdot P_{2,1} \cdot Vh_2 + Vh_3^T \cdot P_{3,1} \cdot Vh_3}{f}} \end{cases} \quad (7)$$

- or for strategy no. 2:

$$\begin{cases} StdB_w = \sqrt{\frac{VB_1^T \cdot P_{1,2} \cdot VB_1 + VB_2^T \cdot P_{2,2} \cdot VB_2 + VB_3^T \cdot P_{3,2} \cdot VB_3}{f}} \\ StdL_w = \sqrt{\frac{VL_1^T \cdot P_{1,2} \cdot VL_1 + VL_2^T \cdot P_{2,2} \cdot VL_2 + VL_3^T \cdot P_{3,2} \cdot VL_3}{f}} \\ Stdh_w = \sqrt{\frac{Vh_1^T \cdot P_{1,2} \cdot Vh_1 + Vh_2^T \cdot P_{2,2} \cdot Vh_2 + Vh_3^T \cdot P_{3,2} \cdot Vh_3}{f}} \end{cases} \quad (8)$$

where: $StdB_W$ – standard deviation of Latitude, $StdL_W$ – standard deviation of Longitude, $Stdh_W$ – standard deviation of ellipsoidal height, $VB_1 = B_1 - B_W$, residuals, difference of Latitude between the weighted mean model and the single GPS/EGNOS solution, calculated separately for strategies no. 1 and 2, $VL_1 = L_1 - L_W$, residuals, difference of Longitude between the weighted mean model and the single GPS/EGNOS solution, calculated separately for strategies no. 1 and 2, $Vh_1 = h_1 - h_W$, residuals, difference of ellipsoidal height between the weighted mean model and the single GPS/EGNOS solution, calculated separately for strategies no. 1 and 2, $VB_2 = B_2 - B_W$, residuals, difference of Latitude between the weighted mean model and the single GPS/UK SBAS solution, calculated separately for strategies no. 1 and 2, $VL_2 = L_2 - L_W$, residuals, difference of Longitude between the weighted mean model and the single GPS/UK SBAS solution, calculated separately for strategies no. 1 and 2, $Vh_2 = h_2 - h_W$, residuals, difference of ellipsoidal height between the weighted mean model and the single GPS/UK SBAS solution, calculated separately for strategies no. 1 and 2, $VB_3 = B_3 - B_W$, residuals, difference of Latitude between the weighted mean model and the single GPS/AL-SBAS solution, calculated separately for strategies no. 1 and 2, $VL_3 = L_3 - L_W$, residuals, difference of Longitude between the weighted mean model and the single GPS/AL-SBAS solution, calculated separately for strategies no. 1 and 2, $Vh_3 = h_3 - h_W$, residuals, difference of ellipsoidal height between the weighted mean model and the single GPS/AL-SBAS solution, calculated separately for strategies no. 1 and 2.

Next mean error of the arithmetic mean [56, 70, 71] for BLh coordinates was estimated as below:

$$\begin{cases} MB_w = \frac{StdB_w}{\sqrt{n}} \\ ML_w = \frac{StdL_w}{\sqrt{n}} \\ Mh_w = \frac{Stdh_w}{\sqrt{n}} \end{cases} \quad (9)$$

where: $StdB_W$ – mean errors of the arithmetic mean of Latitude, calculated separately for strategies no. 1 and 2, $StdL_W$ – mean errors of the arithmetic mean of Longitude, calculated separately for strategies no. 1 and 2, $Stdh_W$ – mean errors of the arithmetic mean of ellipsoidal height, calculated separately for strategies no. 1 and 2.

All algorithms defined by Equations 1–9 were implemented in a numerical script developed in the Scilab v.2024.1.0 environment [72]. The script included computational routines as well as the generation of graphical plots. The numerical analysis was performed using GNSS data collected during the UAV `flight [73] experiment conducted in southern Poland in the spring of 2024. The test flight was carried out in a mountainous area near the town of Tylicz. Figure 3 presents the VTOL WingtraOne UAV before the flight experiment. The flight duration ranged from 09:23:27 (33807 s) to 09:47:44 (35264 s) GPST. Figure 4 shows the horizontal projection of the UAV flight trajectory generated using Google Earth software [74]. Additionally, Figure 5 presents the vertical flight trajectory, with the flight altitude varying between approximately 650 m and 898 m.

RESEARCH RESULTS

After describing the research materials and methods, the obtained research results are presented. First, Figure 6 illustrates the number of GPS satellites for which SBAS corrections were determined for the EGNOS, UK SBAS and AL-SBAS systems. In the case of the GPS/EGNOS solution, the number of satellites ranged from 7 to 10. For the GPS/UK SBAS solution, the number

Figure 3. The UAV before flight experiment

Figure 4. The flight trajectory of UAV [74]

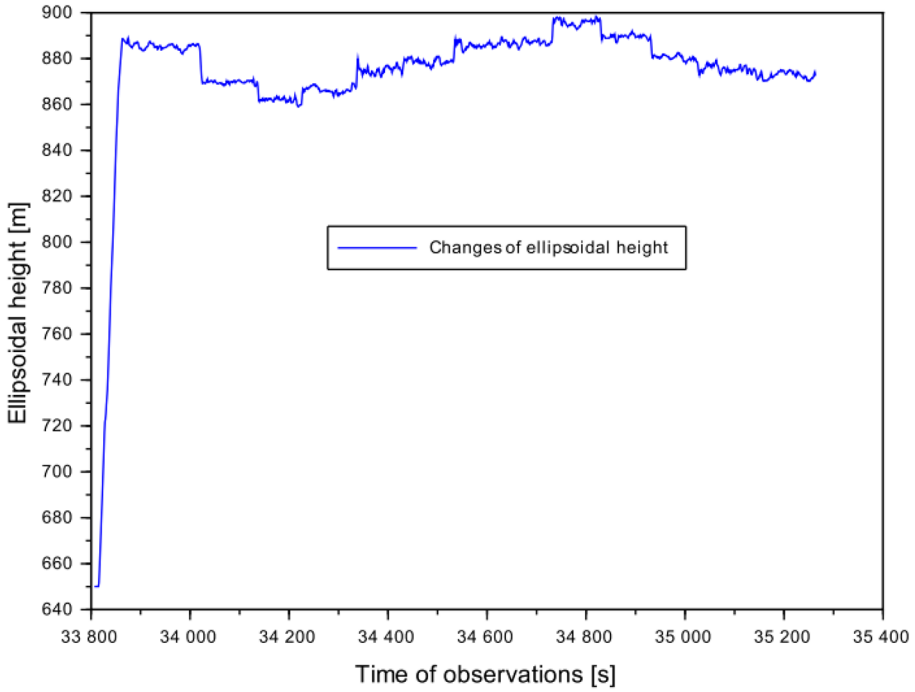

Figure 5. The vertical trajectory of UAV flight

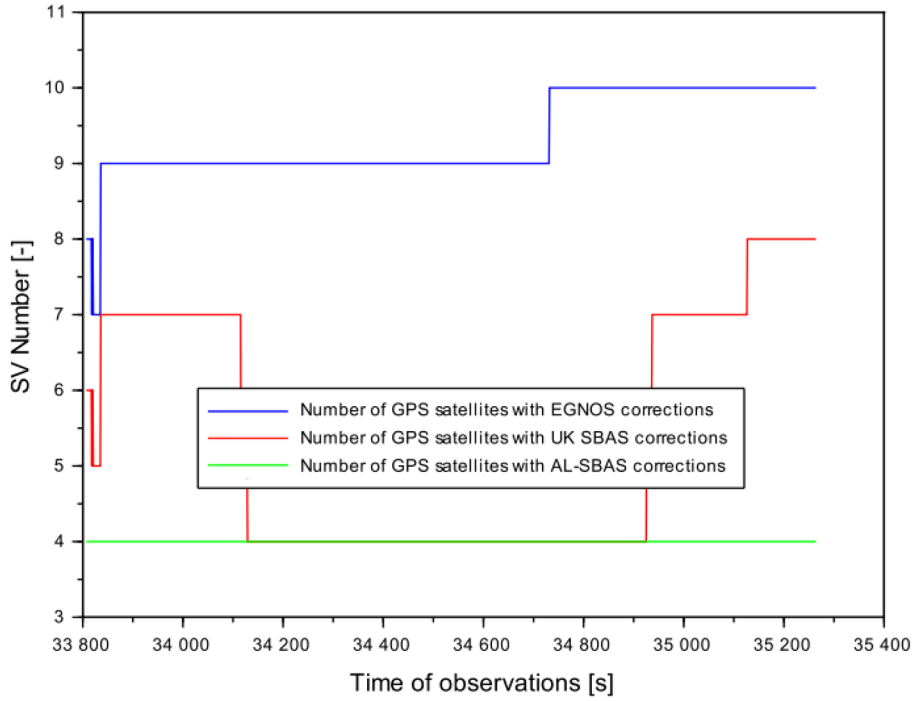

Figure 6. Number of GPS satellites tracked with SBAS corrections

of satellites ranged from 4 to 8. In contrast, the AL-SBAS augmentation system provided corrections for four GPS satellites throughout the entire UAV flight duration. The largest number of GPS satellites with SBAS corrections was observed for the GPS/EGNOS solution, while the smallest number was observed for the GPS/AL-SBAS solution. The largest number of SBAS corrections were determined for GPS satellites in the case of EGNOS, which is not surprising given the long-standing use of this system in air navigation in Poland. The UK SBAS system also generated a significant number of SBAS corrections for GPS satellites, despite being in the validation phase.

The smallest number of SBAS corrections was generated by the AL-SBAS system, due to the availability of a correction model up to a geodetic latitude of 50°. The number of GPS satellites with SBAS corrections directly impacts the calculation of the measurement weight for strategy no. 1, as shown in Figure 7.

By determining the number of GPS satellites with SBAS corrections, it was possible to calculate the measurement weights ($P_{1,1}$, $P_{1,2}$, $P_{3,1}$) for calculation strategy no. 1. Figure 7 presents the obtained results of the measurement weights ($P_{1,1}$, $P_{1,2}$, $P_{3,1}$) for calculation strategy No. 1. The measurement weights are as follows:

- the parameter $P_{1,1}$ changed from 0.100 to 0.143;
- the parameter $P_{2,1}$ varied from 0.125 to 0.250;
- the parameter $P_{3,1}$ was equal to 0.250.

In the case of the results of the parameters ($P_{1,1}$, $P_{2,1}$, $P_{3,1}$), it is necessary to consider the mathematical formula used to determine them and how these results should be interpreted. The smaller the number of satellites, the higher the measurement weights ($P_{1,1}$, $P_{2,1}$, $P_{3,1}$), which is best illustrated by the AL-SBAS system. Conversely, in the case of a large number of satellites, for example in the EGNOS system, the measurement weights ($P_{1,1}$, $P_{2,1}$, $P_{3,1}$) decrease and are the smallest in the analyzed experiment. However, this process should be viewed objectively, as it depends on the number of satellites, which under kinematic flight conditions may change frequently.

Then, Figure 8 shows the results of the point position error ellipsoid parameter calculated within Equation 6. Figure 8 shows the obtained results of the point position error ellipsoid. Thus, the values of the point position error ellipsoid were as follows:

- the parameter CL_1 changed from 2.05 m to 2.63 m;
- the parameter CL_2 changed from 2.88 m to 11.81 m;
- the parameter CL_3 changed from 2.01 m to 16.37 m.

It should be noted that the smallest values of the point position error ellipsoid are observed for the EGNOS system, which indicates that the UAV position coordinates in the single GPS/EGNOS solution were determined with the smallest mean errors. Worse results of the position error ellipsoid can be observed in the case of the GPS/UK SBAS solution. In this case, the value of the parameter CL_2 reaches almost 12 m. What is also important to emphasize is that large values of the point position error ellipsoid in the GPS/UK SBAS solution occur when the number of satellites drops to 4 (see Figure 6). In the GPS/AL-SBAS solution, abrupt jumps in the values of the point position error ellipsoid are visible. This should be explained by the number of tracked

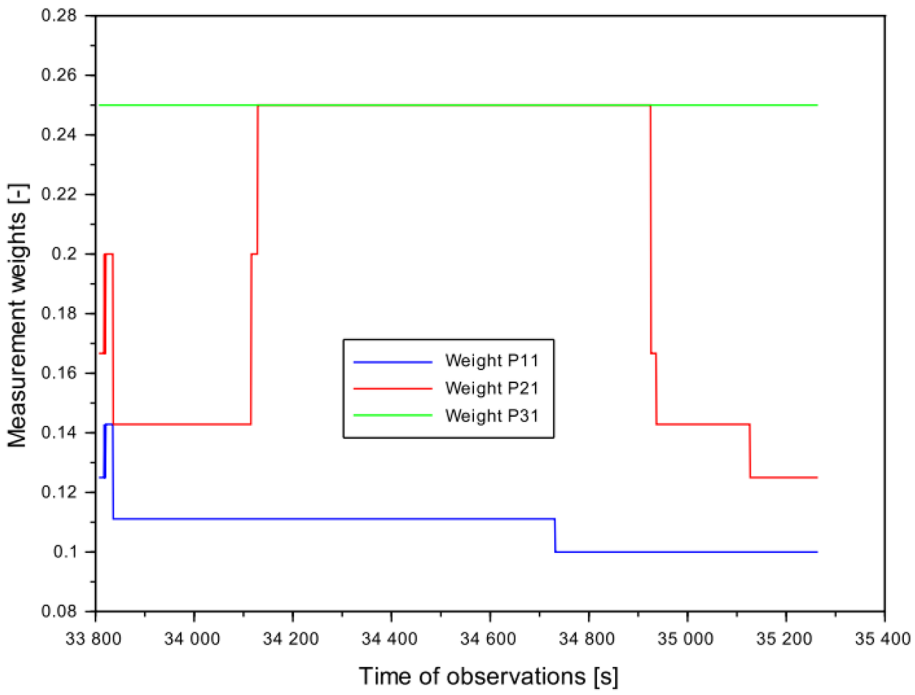

Figure 7. The measurement weights in strategy no. 1

GPS satellites with AL-SBAS corrections, which amounted to 4 throughout the entire UAV flight. In this case, the jumps of the point position error ellipsoid reach even more than 16 m.

By determining the ellipsoid parameter of the point position error, it was possible to calculate the measurement weights ($P_{1,2}$, $P_{2,2}$, $P_{3,2}$) for calculation strategy no. 2. Figure 9 presents the obtained results of the measurement weights ($P_{1,2}$, $P_{2,2}$, $P_{3,2}$) for calculation strategy no. 2. The measurement weights are as follows:

- the parameter $P_{1,2}$ changed from 0.381 to 0.488;

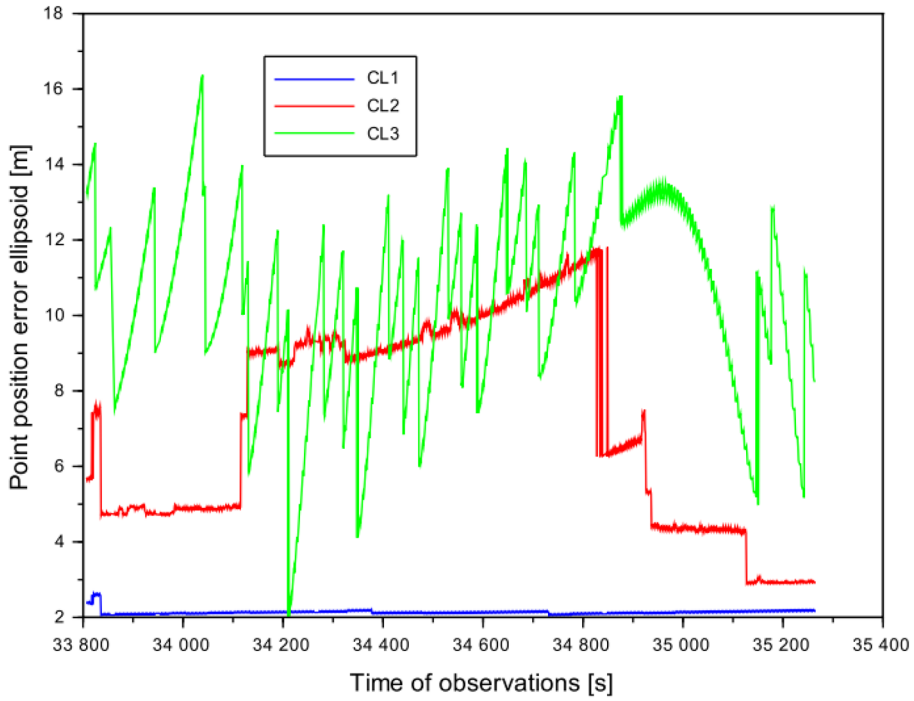

Figure 8. The values of point position error ellipsoid

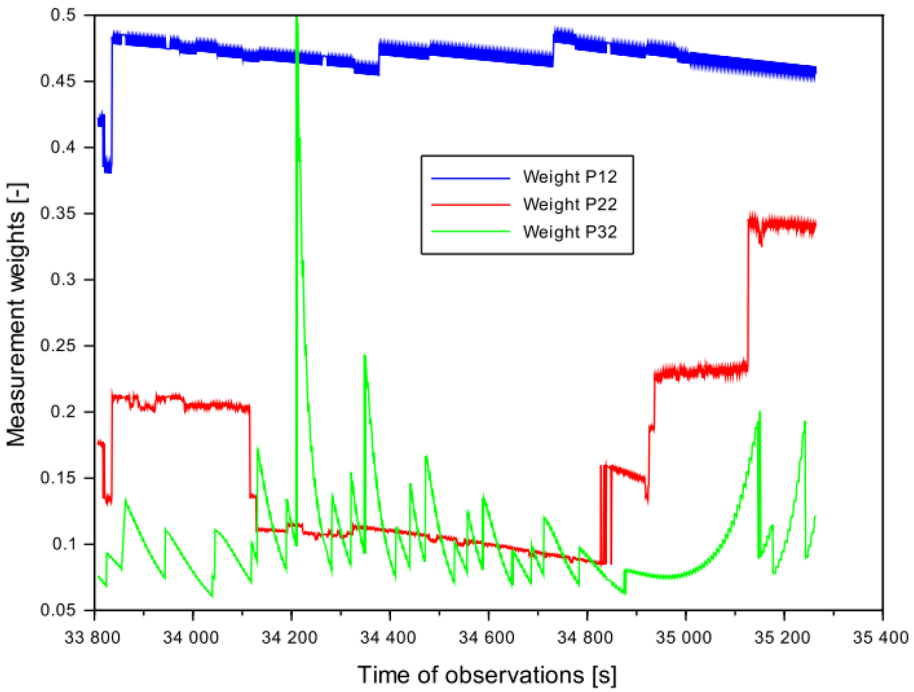

Figure 9. The measurement weights in strategy no. 2

- the parameter $P_{2,2}$ changed from 0.085 to 0.347;
- the parameter $P_{3,2}$ changed from 0.061 to 0.499.

The values presented in Figure 9 are determined using the mathematical Equation 6. Accordingly, the smallest values of the position error ellipsoid correspond to the largest measurement weights ($P_{1,2}$, $P_{2,2}$, $P_{3,2}$). Thus, in the GPS/EGNOS solution, the values of the position error ellipsoid were the smallest, which resulted in large values of the measurement weights $P_{1,2}$. The measurement weights $P_{2,2}$ obtained from the GPS/UK SBAS solution are smaller than the weights $P_{1,2}$ estimated from the GPS/EGNOS solution. In the case of the measurement weights $P_{3,2}$, they assume values ranging from the smallest to the largest within the analyzed dataset. This is caused by frequent changes in the parameter CL_3.

After determining the measurement weights, the precision results of the determined BLh coordinates were presented. First, Figures 10–11 presents the standard deviation results for both calculation strategies no. 1 and 2. In the case of calculation strategy no. 1, the standard deviations of the BLh coordinates were as follows:

- for coordinate B: from 0.05 m to 5.90 m,
- for coordinate L: from 0.03 m to 1.76 m,
- for coordinate h: from 0.16 m to 9.60 m.

In the case of calculation strategy no. 2, the standard deviations of the BLh coordinates were as follows:

- for coordinate B: from 0.06 m to 4.21 m,
- for coordinate L: from 0.04 m to 1.21 m,
- for coordinate h: from 0.23 m to 7.02 m.

Moreover, the arithmetic mean values for the parameters ($StdB_W$, $StdL_W$, $Stdh_W$) are:

- for coordinate B: 1.71 m from strategy no. 1 and 1.43 m from strategy no. 2,
- for coordinate L: 0.37 m from strategy no. 1 and 0.31 m from strategy no. 2,
- for coordinate h: 3.01 m from strategy no. 1 and 2.60 m from strategy no. 2.

By comparing the obtained results of standard deviations, it can be observed that they are smaller in the case of strategy no. 2. This indicates that the measurement weights in strategy no. 2 were better selected than in strategy no. 1.

Having calculated the standard deviations of the BLh coordinates from both calculation strategies, it is now worth comparing them. Such a comparison was implemented using Equation 10. Specifically, Equation 10 compares the percentage of how much better the results from strategy no. 2 are than those from strategy no. 1. Equation 10 is written as:

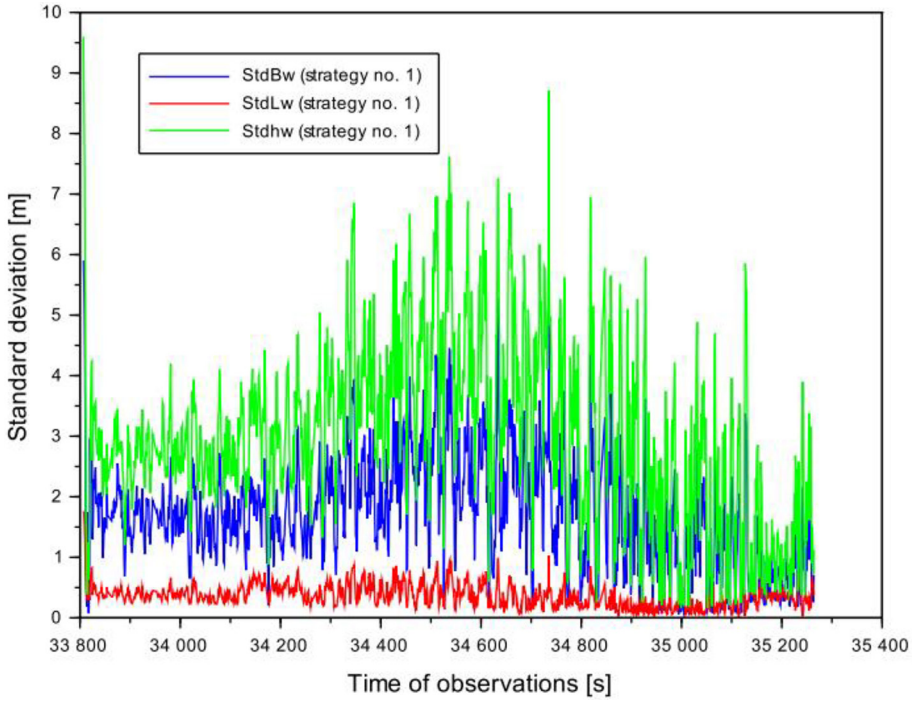

Figure 10. Standard deviation for BLh coordinates based on strategy no. 1

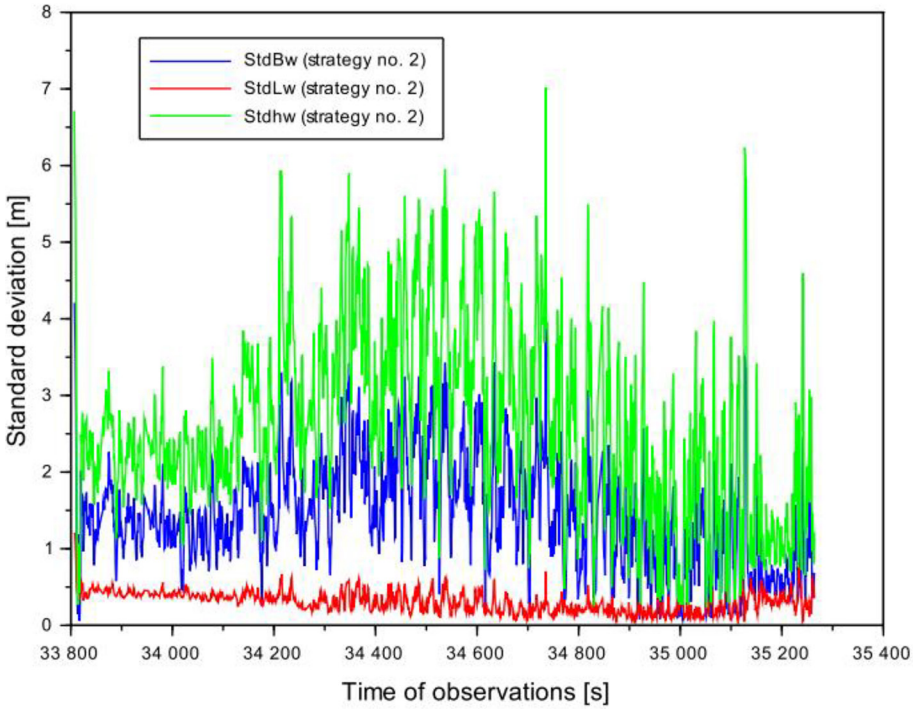

Figure 11. Standard deviation for BLh coordinates based on strategy no. 2

$$\begin{cases} UB[\%] = 100\% \cdot (1 - \frac{mean(StdB_{w,2})}{mean(StdB_{w,1})}) \\ UL[\%] = 100\% \cdot (1 - \frac{mean(StdL_{w,2})}{mean(StdL_{w,1})}) \\ Uh[\%] = 100\% \cdot (1 - \frac{mean(Stdh_{w,2})}{mean(Stdh_{w,1})}) \end{cases} \quad (10)$$

where: UB[%] – percentage value of the increase in the precision determination for component B from strategy no. 2 compared to strategy no. 1, UL[%] – percentage value of the increase in the precision determination for the L component from strategy no. 2 compared to strategy no. 1, *Uh*[%] – percentage value of the increase in the precision determination for the h component from strategy no. 2 compared to strategy no. 1, mean – arithmetic mean value operator, $StdB_{W,1}$ – standard deviations of the determined UAV position for the B component from strategy no. 1 (see Equation 7), $StdL_{W,1}$ – standard deviations of the determined UAV position for the L component from strategy no. 1 (see Equation 7), $Stdh_{W,1}$ – standard deviations of the determined UAV position for the h component from strategy no. 1 (see Equation 7), $StdB_{W,2}$ – standard deviations of the determined UAV position for the B component from strategy no. 2 (see Equation 8), $StdL_{W,2}$ – standard deviations of the determined UAV position for the L component from strategy no. 2 (see Equation 8), $Sth_{W,2}$ – standard deviations of the determined UAV position for the h component from strategy no. 2 (see Equation 8).

For comparison purposes, the standard deviations obtained using computational strategy no. 1 were denoted with subscript 1, whereas those from strategy no. 2 were denoted with subscript 2. The standard deviations for strategy no. 1 were calculated using Equation 7, while those for strategy no. 2 were calculated using Equation 8. Based on the obtained results, it can be concluded that the application of strategy no. 2 improved the determination of the standard deviation of the BLh coordinates by 13% to 17% compared to strategy no. 1. It is worth explaining what such an improvement, expressed as a percentage increase in the determination of the standard deviation, actually means. In fact, an improvement in the determination of the standard deviation implies:

- a better selection of an appropriate weighting strategy for GPS/SBAS observations (see strategy no. 2),
- development of mathematical algorithms based on the weighted mean model for precise GPS + Multi-SBAS positioning,

- a better fitting of the residuals (see Equations 7–8) for individual BLh components, - a better agreement of the coordinates from single GPS/EGNOS, GPS/UK SBAS, and GPS/AL-SBAS solutions with respect to the position calculated using the weighted mean model, - and, in general terms, an increase in the precision of GPS/SBAS positioning.

Finally, Figures 12–13 presents the results of the mean error of the arithmetic mean for the determined BLh coordinates of the UAV position. In the case of calculation strategy no. 1, the mean errors of the arithmetic mean of the BLh coordinates were as follows:

- for coordinate B: from 0.03 m to 3.41 m,
- for coordinate L: from 0.02 m to 1.02 m,

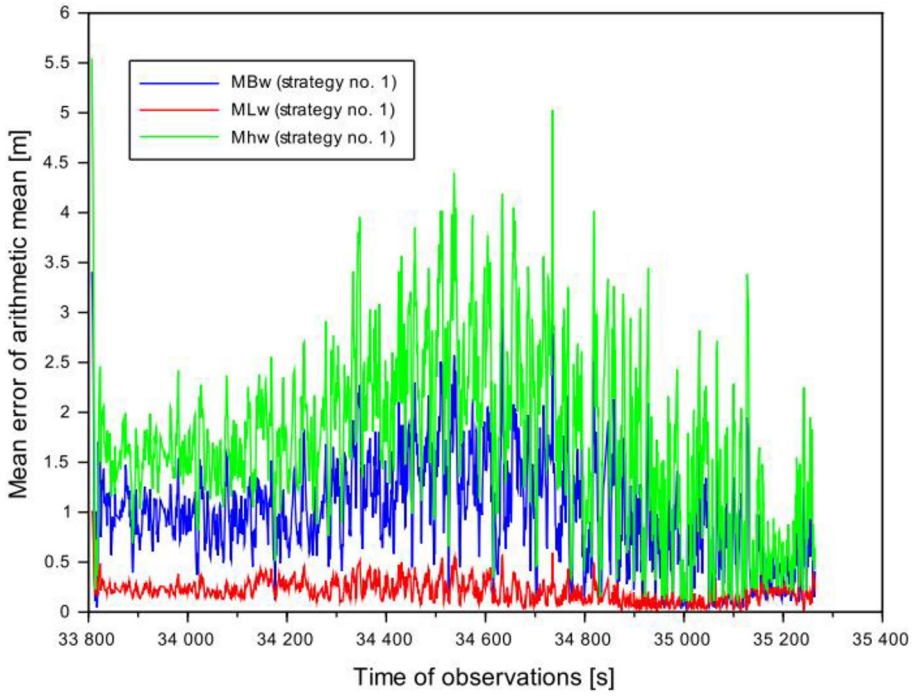

Figure 12. Mean error of arithmetic mean for BLh coordinates based on strategy no. 1

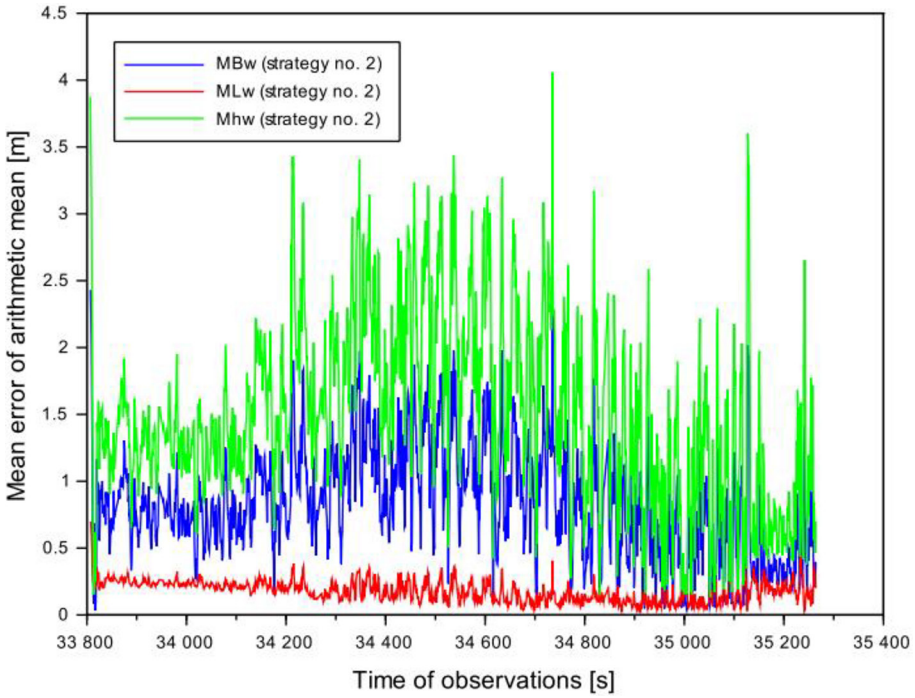

Figure 13. Mean error of arithmetic mean for BLh coordinates based on strategy no. 2

- for coordinate h: from 0.09 m to 5.54 m.

In the case of calculation strategy no. 2, the standard deviations of the BLh coordinates were as follows:

- for coordinate B: from 0.03 m to 2.43 m,
- for coordinate L: from 0.02 m to 0.70 m,
- for coordinate h: from 0.13 m to 4.05 m.

Moreover, the arithmetic mean values for the parameters (MB_W, ML_W, Mh_W) are:

- for coordinate B: 0.99 m from strategy no. 1 and 0.82 m from strategy no. 2,
- for coordinate L: 0.21 m from strategy no. 1 and 0.18 m from strategy no. 2,
- for coordinate h: 1.73 m from strategy no. 1 and 1.49 m from strategy no. 2.

By comparing the obtained results of mean error of the arithmetic mean, it can be observed that they are smaller in the case of strategy no. 2. This indicates that the measurement weights in strategy no. 2 were better selected than in strategy no. 1. Moreover, the values of the mean error of the arithmetic mean are strongly influenced by the results of the standard deviation (see Equation 9). In Equation 9, the variable is the standard deviation, while the denominator of the expression is treated as a constant value.

DISCUSSION

The discussion begins with a comparison of the obtained precision results with those derived using a simple arithmetic mean model [41, 56, 75] within the framework of the proposed integration algorithm expressed by Equations 1–9. In this case, the UAV position coordinates are determined as the arithmetic mean of the individual GPS/EGNOS, GPS/UK SBAS and GPS/AL-SBAS solutions, as expressed by Equation 11:

$$\begin{cases} B_w = \frac{\sum_{i=1}^{n} B_i}{n} \\ L_w = \frac{\sum_{i=1}^{n} L_i}{n} \\ h_w = \frac{\sum_{i=1}^{n} h_i}{n} \end{cases} \tag{11}$$

The corresponding standard deviations are calculated according to Equation 12:

$$\begin{cases} StdB_w = \sqrt{\frac{VB_1^T \cdot VB_1 + VB_2^T \cdot VB_2 + VB_3^T \cdot VB_3}{f}} \\ StdL_w = \sqrt{\frac{VL_1^T \cdot VL_1 + VL_2^T \cdot VL_2 + VL_3^T \cdot VL_3}{f}} \\ Stdh_w = \sqrt{\frac{Vh_1^T \cdot Vh_1 + Vh_2^T \cdot Vh_2 + Vh_3^T \cdot Vh_3}{f}} \end{cases} \tag{12}$$

Figure 14 presents the standard deviation values for the BLh coordinates determined using the arithmetic mean model. The obtained standard

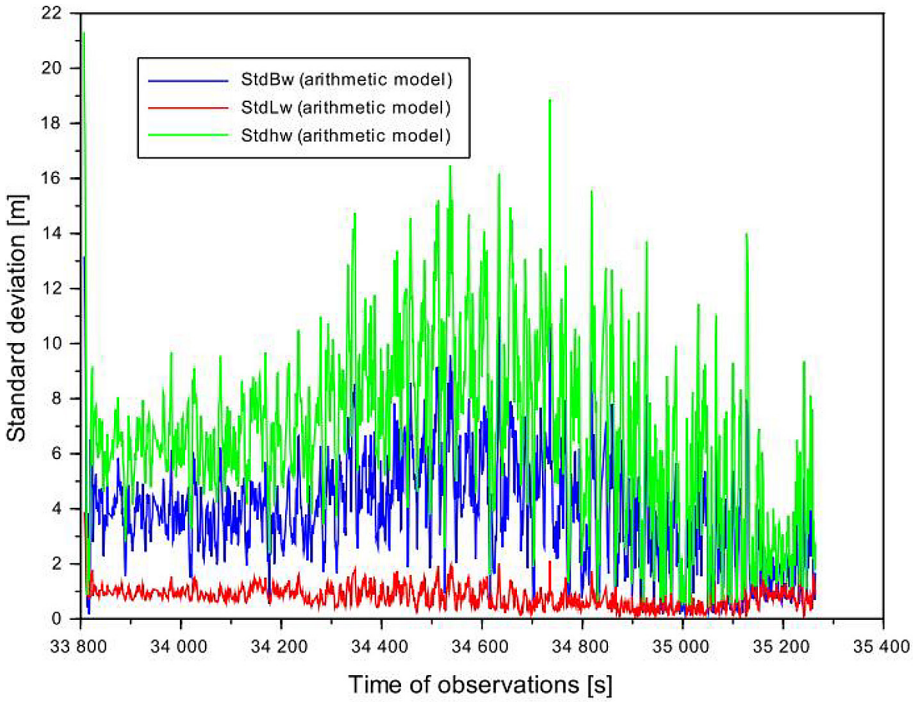

Figure 14. Standard deviation for BLh coordinates based on arithmetic mean model

deviation values ranged from 0.13 m to 13.17 m for the B coordinate, from 0.09 m to 3.88 m for the L coordinate, and from 0.45 m to 21.32 m for the h coordinate. The arithmetic mean values of the standard deviation parameters were equal to 3.82 m for B, 0.82 m for L and 6.79 m for h. Using Equation 12, a comparison of the standard deviation results obtained with the arithmetic mean model and those obtained using the weighted mean integration strategies can be performed. The results indicate that the standard deviation values derived from the arithmetic mean model are significantly worse:

- by approximately 55% for the B coordinate relative to computational strategy no. 1 and 64% relative to computational strategy no. 2,
- by approximately 54% for the L coordinate relative to computational strategy no. 1 and 62% relative to computational strategy no. 2,
- by approximately 56% for the h coordinate relative to computational strategy no. 1 and 61% relative to computational strategy no. 2.

Figure 15 presents the results of the mean error of the arithmetic mean for the BLh coordinates determined using the arithmetic mean model. The obtained values ranged from 0.08 m to 7.60 m for the B coordinate, from 0.05 m to 2.24 m for the L coordinate, and from 0.25 m to 12.31 m for the h coordinate. The arithmetic mean values of the mean error of the arithmetic mean were equal to 2.20 m for B, 0.47 m for L and 3.92 m for h.

The second part of the discussion concerns the determination of the UAV positioning accuracy. For this purpose, the position error parameters were calculated according to Equation 13 [76]:

$$\begin{cases} \Delta B = B_{w,2} - B_{ref} \\ \Delta L = L_{w,2} - L_{ref} \\ \Delta h = h_{w,2} - h_{ref} \end{cases} \tag{13}$$

where: ΔB – position errors along to B coordinate, ΔL – position errors along to L coordinate, Δh – position errors along to h coordinate, $B_{w,2}$ – determined UAV position for the B component from strategy no. 2 (see Equation 8), $L_{w,2}$ – determined UAV position for the L component from strategy no. 2 (see Equation 8), $h_{w,2}$ – determined UAV position for the h component from strategy no. 2 (see Equation 8), B_{ref} – reference coordinate of UAV along B coordinate based on PPK solution, L_{ref} – reference coordinate of UAV along L coordinate based on PPK solution, h_{ref} – reference coordinate of UAV along h coordinate based on PPK solution.

In Equation 13, the coordinates of the determined UAV position are denoted with the

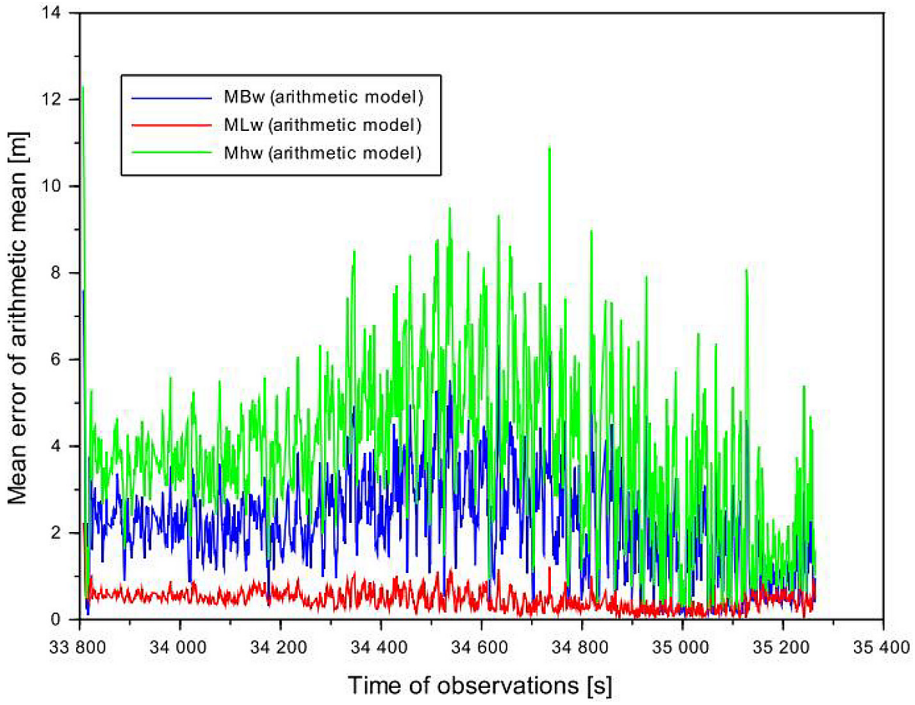

Figure 15. Mean error of arithmetic mean for BLh coordinates based on arithmetic mean model

subscript 2, which in practice indicates that they were calculated using strategy no. 2. Position errors involve comparing the determined UAV position coordinates with the flight reference position. The determined UAV coordinates obtained from computational strategy no. 2 were used for the comparison, as this method yielded the best precision results. Furthermore, the flight reference position was calculated using the PPK method [77] with an accuracy better than 0.028 m for all BLh components [78]. The flight reference position was determined using MAGNET Tools v.5.1.1.0 [79]. Figure 16 shows the results of position errors (ΔB, ΔL, Δh). The position errors ranged from 0.14 m to 4.59 m for ΔB, from -0.27 m to 1.09 m for ΔL, and from -4.48 m to 0.22 m for Δh. The smallest position errors are for the parameter ΔL, and the largest for the parameters (ΔB, Δh).

The third part of the discussion concerns a general summary of the conducted research, measurement conditions, and the testing conditions of the research method. It should be emphasized that the best solution was obtained for strategy no. 2, i.e., weighting as a function of the inverse of the point position error ellipsoid. This weighting process proved to be more effective than weighting based on the inverse of the number of tracked satellites. As shown in the literature, GNSS measurement weighting should be performed using mathematical formulas based on the mean observation errors [80, 81]. Thus, in the classical approach, measurement weighting can be implemented as a function of the inverse of the square of the mean error [82]. However, in the present study, the weighting approach was modified and based on the inverse of the point position error ellipsoid. This results in each BLh component having the same measurement weight at a given epoch in a single GPS/SBAS solution (e.g., GPS/EGNOS). Consequently, each BLh position component has an equal measurement weight at a given epoch. This is significant in kinematic tests, as the BLh position changes every 1 s, yet the measurement weight remains the same in a single GPS/SBAS solution. When the mathematical model is extended and effectively based on three single GPS/SBAS solutions, nine individual mean error results are obtained. Therefore, it was necessary to optimize the weighting process and select measurement weights that are compatible with the proposed algorithm (1–9).

A separate aspect of this part of the discussion is the analysis of geometric conditions and signal availability during the flight mission. In this case, positioning was based on GPS satellites and the L1-C/A code signal, as all SBAS systems generated corrections for the GPS navigation system, which is consistent with the commonly applicable ICAO standards for civil aviation applications [4].

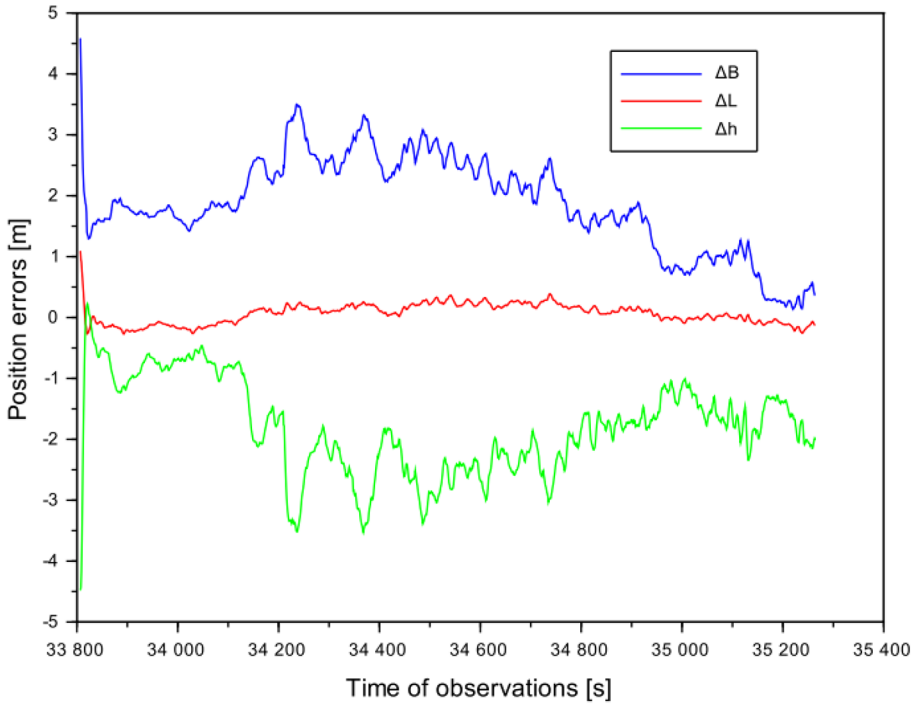

Figure 16. Positioning errors of UAV vehicle

The presented research method can be used if and only if both the GPS signal and SBAS corrections are available. Otherwise, the availability of a UAV position navigation solution is not possible. A significant advantage of the proposed method is that in the event of the loss of corrections from one SBAS system, the algorithm can still operate using the remaining two SBAS systems. However, in such a case, the position solution will have a degree of freedom equal to 1. Robustness with respect to satellite geometry must be based on at least four tracked GPS satellites for which SBAS corrections have been generated. Naturally, the higher the number of GPS satellites, the lower the DOP geometric coefficients become [76]. Nevertheless, for the position navigation solution to be feasible, at least four GPS satellites must be available at each measurement epoch in order for the algorithm to operate. These constitute the minimum satellite geometry requirements. At this point, it is worth referring directly to the research results for the GPS/AL-SBAS solution, in which four GPS satellites with AL-SBAS corrections were available. The solvability condition was satisfied, as at least four pseudorange measurements were available to determine the coordinates. However, it can be inferred that if the number of GPS satellites with AL-SBAS corrections were higher, the quality of the coordinate determination obtained using algorithm (1–9) would likely be even better.

With further reference to the measurement conditions, it should be noted that the study concerns only a single selected UAV flight. Therefore, there is no repeatability of the measurement and computational processes. Within the measurement process, a major limitation is the requirement to equip the UAV with an appropriate GNSS receiver capable of recording GPS observations as well as SBAS corrections. Access to corrections is particularly important; thus, the given SBAS augmentation system must be operational. Moreover, in the case of the GPS navigation system, the receiver must record code-based measurements on the L1 frequency. The flight was conducted in mountainous terrain, which resulted in a relatively high UAV flight altitude. In lowland areas, the altitude ceiling would be significantly lower. Additionally, UAV operations in mountainous regions are constrained by weather conditions, such as strong wind gusts. Therefore, UAV flights should preferably be conducted under calm and windless weather conditions.

Finally, within this discussion thread, it is worth addressing the testing conditions of the presented research method. The developed mathematical algorithms (1–9) can be applied both in real-time operation and in post-processing mode. The boundary condition is that the UAV must be equipped with an appropriate GPS receiver capable of receiving GPS signals and SBAS corrections. In real-time operation, maintaining continuity of positioning and GNSS data availability is crucial. With regard to continuity, it is necessary to verify whether there are any interruptions in the UAV position navigation solution, which essentially comes down to checking whether the coordinates are determined at 1 s intervals. In terms of availability, the GPS L1 signal and the coverage of SBAS corrections must be verified. The absence of any of these elements would hinder real-time UAV navigation using the developed algorithm (1–9).

The last part of the discussion addresses a comparison of the proposed research methodology with existing studies reported in the literature. Similar to previous works [8–10], this study applies SBAS augmentation systems such as EGNOS, UK SBAS and AL-SBAS. Moreover, the determination of UAV coordinates and their precision follows approaches presented in [41], while positioning accuracy assessment is consistent with methodologies applied in [5, 8]. The use of UAV technology aligns with research reported in [2]. The main advantage of the proposed approach lies in the simultaneous use of corrections from three SBAS augmentation systems, in contrast to studies [11, 12], where only two SBAS systems were considered. An additional contribution is the development of a position determination algorithm that integrates corrections from multiple SBAS systems instead of relying on a single SBAS solution, as reported in [1]. Furthermore, the comparison of two independent computational strategies represents a novel aspect compared to [56]. Finally, the results demonstrate that weighting based on the inverse of the point position error ellipsoid provides superior performance compared to other weighting approaches, which differs from the conclusions reported in [57].

CONCLUSIONS

The article presents the results of research concerning the determination of kinematic UAV position coordinates, as well as their precision

and accuracy. The study uses GPS code-based signals and corrections from three augmentation systems: EGNOS, UK SBAS, and AL-SBAS. The research material consisted of GNSS data collected during a UAV flight experiment conducted in southern Poland in the spring of 2024. The experiment was performed using a VTOL WingtraOne UAV equipped with a NovAtel OEM7500 GNSS receiver. Data processing was carried out using RTKLIB v.2.4.3, MAGNET Tools v.5.1.1.0 and Scilab 2024.1.0 software. The main methodological conclusions can be summarized as follows:

- show new approach to kinematic user positioning based on the integration of SBAS corrections from three augmentation systems: EGNOS, UK SBAS, and AL-SBAS,
- development new algorithm for determining the user position based on the combination of navigation solutions obtained from individual SBAS systems,
- proposed algorithm applies a weighted mean model using two independent computational strategies,
- in computational strategy no. 1, the measurement weights are defined as the inverse of the number of tracked satellites, whereas in computational strategy no. 2, the weights are defined as the inverse of the point position error ellipsoid.

Among the practical conclusions, the following can be distinguished:

- demonstration that the most effective computational strategy in the presented algorithm is weighting based on the inverse of the point position error ellipsoid,
- demonstration that the use of a weighted mean model in the presented algorithm is superior to the arithmetic mean model,
- achievement of the best precision and accuracy results for computational strategy no. 2,
- advancement of GPS + Multi-SBAS positioning for high-precision UAV positioning.

Possible limitations of the study may concern the continuity of kinematic UAV positioning as well as the availability of GPS data and SBAS corrections from three augmentation systems: EGNOS, UK SBAS, and AL-SBAS. Therefore, both the GPS navigation system and the aforementioned SBAS systems must be operational at the time of UAV flight execution. Most importantly, the onboard GNSS receiver must be capable of receiving GPS code-based signals and SBAS corrections in real time. The presented research methodology can be applied to other SBAS augmentation systems operating in regions with overlapping correction coverage. Furthermore, the proposed approach may be extended to land and maritime navigation applications within the transportation domain. Future research may focus on real-time implementation of the proposed algorithm, the use of multi-constellation GNSS observations, and the assessment of integrity parameters for safety-critical navigation applications. Therefore, it is necessary to conduct further UAV flights in order to verify the developed algorithm (1–9). In future studies, the proposed algorithm may be extended to determine additional SBAS positioning quality parameters used in aviation, namely availability, continuity, and integrity, as well as to compute protection levels (HPL/VPL) within the framework of SBAS APV approach procedures. This is particularly relevant since the determination of SBAS positioning quality parameters in aviation will be based on a Multi-SBAS solution. At this stage, the Multi-SBAS solution was implemented for the GPS navigation system; however, SBAS corrections can also be adapted for other global navigation satellite systems GNSS.

REFERENCES

1. Grzegorzewski M. Navigating an aircraft by means of a position potential in three dimensional space, Annual of Navigation, 2005, 9, 1–111.
2. Krasuski K. Algorithms for improving GPS/SBAS positioning accuracy using EGNOS and SDCM augmentation systems, Polish Air Force University Publishing House, 2025, 1–147, https://doi.org/10.55676/68629-06-4 (in Polish)
3. Grzegorzewski M., Świątek A., Ciećko A., Oszczak S., Ćwiklak J. Study of EGNOS safety of life service during the period of solar maximum activity, Artificial Satellites, 2012, 47, 137–145, https://doi.org/10.2478/v10018-012-0019-5
4. International Civil Aviation Organization. ICAO standards and recommended practices (SARPS), 2006, I, Annex 10, (Radio Navigation Aids). Available from: http://www.ulc.gov.pl/pl/prawo/prawomi%C4%99dzynarodowe/206-konwencje. (Accessed: 30.12.2025).
5. Ciećko A., Grunwald G. Examination of autonomous GPS and GPS/EGNOS integrity and accuracy for aeronautical applications. Periodica Polytechnica

Civil Engineering. 2017, 61(4), 920–928, https://doi.org/10.3311/PPci.10022

6. IGS MGEX website. Available from: https://igs.org/mgex/constellations/#sbas, (Accessed: 30.12.2025).
7. ESA webiste. Available from: https://www.esa.int/ESA_Multimedia/Images/2023/09/SBAS_coverage, (Accessed: 30.12.2025).
8. Ciećko A., Grzegorzewski M., Ćwiklak J., Oszczak S., Jafernik H. Air navigation in eastern Poland based on EGNOS. In: Proceedings of the Aviation Technology, Integration, and Operations Conference (ATIO 2013), Los Angeles, CA, USA, 12–14 August 2013; Red Hook: Curran, NY, USA, Volume 1, 603–613, https://doi.org/10.2514/6.2013-4254
9. Hill D., Newton G., Soddu C., Dumville M., Easom M., Tiwari S., Roberts W., Lerma J. B., Pericacho J. G., Emes C. A United Kingdom Space-Based Augmentation System Testbed Capability, In: Proceedings of the 35th International Technical Meeting of the Satellite Division of The Institute of Navigation (ION GNSS+ 2022), Denver, Colorado, September 2022, 714-724, https://doi.org/10.33012/2022.18406
10. Lahouaria T., Salem K., Chahrazed D., Younes A., Abdelkrim A. AL-SBAS and EGNOS/GPS Performance for Cartographic Application in Africa, In: Proceedings of the 2023 International Conference on Earth Observation and Geo-Spatial Information (ICEOGI), Algiers, Algeria, 2023, 1–4, https://doi.org/10.1109/ICEOGI57454.2023.10292963
11. Krasuski K., Mrozik M., Wierzbicki D., Ćwiklak J., Kozuba J., Ciećko A. Designation of the quality of EGNOS+SDCM satellite positioning in the approach to landing procedure, Applied Sciences, 2022, 12, 1335, https://doi.org/10.3390/app12031335
12. Krasuski K., Lalak M., Gołda P., Ciećko A., Grunwald G., Mrozik M., Kozuba J. Analysis of the precision of determination of aircraft coordinates using EGNOS+SDCM solution, Archives of Transport, 2023, 67(3), 105–117, https://doi.org/10.5604/01.3001.0053.7264
13. Mrozik M., Kozuba J., Krasuski K., Ćwiklak J., Bakuła M., Ciećko A., Grunwald G., Wierzbicki D. Analysis of the accuracy of EGNOS+SDCM positioning in aerial navigation, Archives of Transport, 2022, 64(4), 135–144, https://doi.org/10.5604/01.3001.0016.2028
14. Krasuski K., Wierzbicki D. Monitoring Aircraft Position Using EGNOS Data for the SBAS APV Approach to the Landing Procedure, Sensors, 2020, *20,* 1945, https://doi.org/10.3390/s20071945
15. Oliveira J., Tiberius C. Landing: Added Assistance to Pilots on Small Aircraft Provided by EGNOS, In Proceedings of the Conference 2008 IEEE/ION Position, Location and Navigation Symposium, Monterey, CA, USA, 5–8 May 2008, 321–333, https://doi.org/10.1109/PLANS.2008.4570021
16. Secretan H., Ventura-Traveset J., Toran F., Solari G., Basker S. EGNOS System Test Bed Evolution and Utilisation, In: Proceedings of the 14th International Technical Meeting of the Satellite Division of The Institute of Navigation (ION GPS 2001), Salt Lake City, UT, USA, 11–14 September 2001, 1891–1900.
17. Azoulai L., Virag S., Leinekugel-Le-Cocq R., Germa C., Charlot B., Durel P. Experimental Flight Tests with EGNOS on A380 to Support RNAV LPV Operations, In: Proceedings of the 22nd International Technical Meeting of The Satellite Division of the Institute of Navigation (ION GNSS 2009), Savannah, GA, USA, 22–25 September 2009, 1203–1215.
18. Breeuwer E., Farnworth R., Humphreys P., Mcgregor A., Michel P., Secretan H., Leighton S. J., Ashton K. J. Flying EGNOS: The GNSS-1 Testbed, Paper Galileo's World, January 2000, 10–21, http://www.egnos-pro.esa.int/Publications/navigation.html, (Accessed: 30.12.2025).
19. Fonseca A., Azinheira J., Soley S. Contribution to the operational evaluation of EGNOS as an aeronautical navigation system, In: Proceedings of the 25th International Congress of the Aeronautical Sciences (ICAS 2006), Hamburg, Germany, 3–8 September 2006, 1–10.
20. Veerman H. P. J., Rosenthal P. EGNOS Flight Trials, Evaluation of EGNOS Performance and Prospects, In Proceedings of the 2006 National Technical Meeting of The Institute of Navigation, Monterey, CA, USA, 18–20 January 2006, 358–367.
21. Ciećko A., Grzegorzewski M., Oszczak S., Ćwiklak J., Grunwald G., Balint J., Szabo S. Examination of EGNOS Safety-of-Live service in Eastern Slovakia, Annual of Navigation, 2015, 22, 65–78, https://doi.org/10.1515/aon-2015-0021
22. Soley S., Farnworth R., Breeuwer E. Approaching nice with the EGNOS system test bed, In: Proceedings of the ION NTM 2002, San Diego, CA, USA, 28–31 January 2002, 539–550.
23. Butzmuehlen C., Stolz R., Farnworth R., Breeuwer E. PEGASUS–Prototype Development for EGNOS Data Evaluation–First User Experiences with the EGNOS System Test-Bed, In: Proceedings of the 2001 National Technical Meeting of The Institute of Navigation, Long Beach, CA, USA, 22–24 January 2001, 628–637.
24. Perrin O., Scaramuzza M., Buchanan T., Brocard D. Flying EGNOS approaches in the Swiss Alps, Journal of Navigation, 2006, 59(2), 177–185, https://doi.org/10.1017/S0373463306003754
25. Muls A., Boon F. Evaluating EGNOS augmentation on a military helicopter, In: Proceedings of the 14th International Technical Meeting of the Satellite Division of The Institute of Navigation (ION GPS

2001), Salt Lake City, UT, USA, 11–14 September 2001, 2458–2462.

26. Hvezda M. Simulation of EGNOS satellite navigation signal usage for aircraft LPV precision instrument approach, Aviation, 2021, 25, 171–181, https://doi.org/10.3846/aviation.2021.14554
27. Vassilev B. Vassileva B., EGNOS performance before and after applying an error extraction methodology, Annual of Navigation, 2012, 19, 121–130, https://doi.org/10.2478/v10367-012-0022-8
28. Lupsic B., Takács B. Analysis of the EGNOS ionospheric model and its impact on the integrity level in the central Eastern Europe region, In: The International Archives of Photogrammetry, Remote Sensing and Spatial Information Sciences; vol. XLII-4/W14, FOSS4G 2019 – Academic Track, 26–30 August 2019, Bucharest, Romania, 159-165, https://doi.org/10.5194/isprs-archives-XLII-4-W14-159-2019
29. Nie Z., Zhou P., Liu F., Wang Z., Gao Y. Evaluation of orbit, clock and ionospheric corrections from five currently available SBAS L1 services: Methodology and Analysis, Remote Sensing, 2019, 11, 411, https://doi.org/10.3390/rs11040411
30. Tabti L., Kahlouche S., Benadda B., Beldjilali B. Improvement of single-frequency GPS positioning performance based on EGNOS corrections in Algeria, Journal of Navigation, 2020, 73(4), 846–860, https://doi.org/10.1017/S037346331900095X
31. Alarcón F., Viguria A., Vilardaga S., Montolio J., Soley S. EGNOS-based Navigation and Surveillance System to Support the Approval of RPAS Operations, In: Proceedings of the 9th SESAR Innovation Days, Athens, Greece, 2–6 December 2019, 1-8.
32. Balsi M., Prem S., Williame K., Teboul D., Délétraz L., Hebrard Capdeville P. I. Establishing new foundations for the use of remotely-piloted aircraft systems for civilian applications. The International Archives of the Photogrammetry, Remote Sensing and Spatial Information Sciences, 2019, 2, 197–201, https://doi.org/10.5194/isprs-archives-XLII-2-W13-197-2019.
33. Geister R., Limmer L., Rippl M., Dautermann T. Total system error performance of drones for an unmanned PBN concept, In: Proceedings of the IEEE Integrated Communications, Navigation, Surveillance Conference (ICNS 2018), Herndon, VA, USA, 10–12 April 2018, 2D4-1–2D4-9, https://doi.org/10.1109/ICNSURV.2018.8384845
34. Pullen S., Enge P., Lee J. Local-Area Differential GNSS Architectures Optimized to Support Unmanned Aerial Vehicles (UAVs), In: Proceedings of the International Technical Meeting of the Institute of Navigation (ION ITM 2013), San Diego, CA, USA, 28–30 January 2013, 559–571.
35. Watanabe Y., Manecy A., Hiba A., Nagai S., Shin A. Vision-integrated navigation system for aircraft final approach in case of GNSS/SBAS or ILS failures, In: Proceedings of the AIAA Scitech Forum 2019, San Diego, CA, USA, 7–11 January 2019; 1-21, https://doi.org/10.2514/6.2019-0114
36. Yoon H., Seok H., Lim C., Park B. An Online SBAS Service to Improve Drone Navigation Performance in High-Elevation Masked Areas, Sensors, 2020, 20, 3047, https://doi.org/10.3390/s20113047
37. González Merino J., Bravo Llano F., Pattinson M., Easom M., Campano Hernández J.R., Sanz Palomar I., Romero Llapa M.I., Priya Ilamparithi S., Hill D., Newton G. UKSBAS testbed performance assessment of two years of operations, Eng. Proc., 2025, 88, 35, https://doi.org/10.3390/engproc2025088035
38. Tabti L., Kahlouche S. Characteristics and performance of Algerian Satellite Based Augmentation System (AL-SBAS). In: Proceedings of the 15th International Conference on Advances in Satellite and Space Communications (SPACOMM 2023), 24-28 April 2023, Venice, Italy, 10–14.
39. Unoosa webiste. Available from: https://www.unoosa.org/documents/pdf/icg/2023/ICG-17/icg17.03.01.pdf, (Accessed: 30.12.2025).
40. Kahlouche S., Tabti L., Benbouzid A. B., Outamazirt F. Algerian Satellite Based Augmentation System Based on Alcomsat-1: Characteristics and Preliminary Performance Tests. In: Proceedings of the United Nations International Meeting on the Application of Global Navigation Satellite Systems, 5–9 December 2022, Vienna, Austria, 1–2.
41. Mrozik M. Application of the SBAS positioning method in the aircraft approach procedure (in Polish). PhD Thesis, Silesian University of Technology, Gliwice, 2023, 1–147.
42. Krasuski K. The research of accuracy of aircraft position using SPP code method (in Polish). Ph.D. Thesis, Warsaw University of Technology, Warsaw, Poland, 2019, 1–106.
43. Fellner R. Analysis of the EGNOS/GNSS parameters in selected aspects of Polish transport. Transport Problems, 2014, 4(9), 27–37.
44. Fellner A., Fellner R., Piechoczek E. Pre-flight validation RNAV GNSS approach procedures for EPKT in "EGNOS APV Mielec project", Scientific Journal of Silesian University of Technology. Series Transport, 2016, 90, 37–46, https://doi.org/10.20858/sjsutst.2016.90.4.
45. Fellner A., Jafernik H. Airborne measurement system during validation of EGNOS/GNSS essential parameters in landing, Reports on Geodesy and Geoinformatics, 2014, 96, 27–37, https://doi.org/10.2478/rgg-2014-0004
46. Kaleta W. EGNOS based APV procedures development possibilities in the south-eastern part of Poland. Annual of Navigation, 2014, 21, 85–94,

https://doi.org/10.1515/aon-2015-0007

47. Skorupski J., Kaleta W. A fuzzy inference approach to analysis of LPV-200 procedures influence on air traffic safety, Transportation Research Part C-Emerging Technologies, 2019, 106, 264–280, https://doi.org/10.1016/j.trc.2019.07.001
48. Siergiejczyk M., Krzykowska K., Rosiński A. Evaluation of the influence of atmospheric conditions on the quality of satellite signal. In: Proceedings of the 12th International Conference on Marine Navigation and Safety of Sea Transportation (TransNav 2017), Gdynia, Poland, 2017, 95–103, https://doi.org/10.1201/9781315099132-20
49. Krzykowska K., Krzykowski M. Forecasting parameters of satellite navigation signal through artificial neural networks for the purpose of civil aviation, International Journal of Aerospace Engineering, 2019, Article ID 7632958, 11, https://doi.org/10.1155/2019/7632958
50. Kirschenstein M., Krasuski K., Goś A. Designating the error of vertical coordinate of aircraft position in the GPS system, Scientific Journal of Silesian University of Technology. Series Transport, 2020, 108, 85-94, https://doi.org/10.20858/sjsutst.2020.108.8
51. Krzykowska-Piotrowska K., Dudek E., Wielgosz P., Milanowska B., Batalla J. M. On the correlation of solar activity and troposphere on the GNSS/EGNOS integrity. Fuzzy Logic Approach, Energies, 2021, 14*,* 4534, https://doi.org/10.3390/en14154534
52. Fellner A., Sulkowski J., Tróminski P., Zadrąg P. The use of reference systems for UAV flight routing, Geophysical Research Abstracts, 2012, 14, EGU2012-6434.
53. Grunwald G., Ciećko A., Kozakiewicz T., Krasuski K. Analysis of GPS/EGNOS positioning quality using different ionospheric models in UAV Navigation, Sensors, 2023, *23,* 1112, https://doi.org/10.3390/s23031112
54. Lalak M., Krasuski K., Wierzbicki D. Methodology to improve the accuracy of determining the position of UAVs equipped with single-frequency receivers for the purposes of gathering data on aviation obstacles, Scientific Journal of Silesian University of Technology. Series Transport, 2023, 119, 83-104, https://doi.org/10.20858/sjsutst.2023.119.5
55. Krasuski K., Wierzbicki D., Lalak M., Ciećko A. Algorithms for improving the position determination of an UAV equipped with a single-frequency GPS receiver for low-altitude photogrammetry, Metrology and Measurement Systems, 2023, 30(3), 441–459, https://doi.org/10.24425/mms.2023.146423
56. Krasuski K., Wierzbicki D., Bakuła M. Improvement of UAV positioning performance based on EGNOS+SDCM solution, Remote Sensing*,* 2021, *13*, 2597, https://doi.org/10.3390/rs13132597
57. Krasuski K., Wierzbicki D. Application the SBAS/EGNOS corrections in UAV positioning, Energies, 2021, 14, 739, https://doi.org/10.3390/en14030739
58. Miduch P., Krasuski K., Ciećko A., Żukowska M., Grzegorzewski M. Application of Kalman filter in accuracy analysis of GPS+UK SBAS positioning in aerial navigation, In: Proceedings of the International Scientific Conference Air Traffic Engineering, 8-9 April 2025, Warsaw, 40–41.
59. Romero I. RINEX version 3.05, 2020. Available from: https://files.igs.org/pub/data/format/rinex305.pdf, (Accessed: 30.12.2025).
60. ESA Navipedia website. Available from: https://gssc.esa.int/navipedia/index.php/The_EGNOS_SBAS_Message_Format_Explained, (Accessed: 30.12.2025).
61. RTKLIB webiste. Avialable from: http://rtklib.com/, (Accessed: 30.12.2025).
62. Krasuski K., Bakuła M., Ciećko A., Grunwald G., Gołda P., Mrozik M., Kozuba J. Algorithms to improve unmanned aerial vehicle positioning accuracy using European geostationary navigation overlay service and system for differential corrections and monitoring ionospheric corrections. Advances in Science and Technology Research Journal. 2025, 19(1), 284–300, https://doi.org/10.12913/22998624/195195
63. Investopedia website. Available from: https://www.investopedia.com/terms/d/degrees-of-freedom.asp, (Accessed: 30.12.2025).
64. Geoforum website. Available from: https://geoforum.pl/upload/pearl/file_2/zeszyt_1.pdf, (Accessed: 30.12.2025).
65. Jaworski J. M. An inaccuracy of the point coordinations in the euclidean space (in Polish). Zeszyty Naukowe Politechniki Śląskiej. Seria: Elektryka, 2005, 195, 91–100.
66. Brach M. Accuracy analysis for determination of coordinates by the selected GNSS receivers in the forest environment, Sylwan, 2012, 156(1), 47−56.
67. Gargula T. Adjustment of an integrated geodetic network composed of GNSS vectors and classical terrestrial linear pseudo-observations. Appl. Sci., 2021, 11, 4352, https://doi.org/10.3390/app11104352
68. Paziewski J., Krukowska M. Ultra fast static GNSS positioning with GPS and Galileo systems, Biuletyn WAT, 2014, 63(2), 89–101.
69. Suda J. Misstatements of GPS-location of public transport vehicles in Warsaw, Przegląd Komunikacyjny, 2017, 72(2), 25–30.
70. Habibzadeh F. On using standard deviation or standard error of the mean, Iran J. Med. Sci., 2025, 50(5), 274–277, https://doi.org/10.30476/ijms.2025.106283.4041

71. Wlodarczyk–Sielicka M., Stateczny A. Clustering bathymetric data for electronic navigational charts, Journal of Navigation, 2016, 69(5), 1143–1153, https://doi.org/10.1017/S0373463316000035
72. Scilab webiste. Available from: https://www.scilab.org/, (Accessed: 30.12.2025).
73. Wingtra website. Available from: https://wingtra.com/mapping-drone-wingtraone/technical-specifications/, (Accessed: 30.12.2025).
74. Google Earth website. Available from: https://earth.google.com/web/@49.39702304,21.03098433,583.6193321a,4993.93010994d,35y,0h,0t,0r/data=CgRCAggBOgMKATBCAggASggIm7GL4wQQAA, (Accessed: 30.12.2025).
75. Skibicki J., Wilk A., Koc W., Licow R., Szmagliński J., Chrostowski P., Judek S., Karwowski K., Grulkowski S. Reducing the uncertainty of the moving object location measurement with the method of quasi-multiple measurement in GNSS Technology in Symmetrical Arrangement. Sensors, 2023, 23, 2657, https://doi.org/10.3390/s23052657
76. Specht M. Experimental studies on the relationship between HDOP and position error in the GPS system. Metrology and Measurement Systems. 2022, 29(1), 17–36, https://doi.org/10.24425/mms.2022.138549
77. Pirti A. Evaluating the accuracy of post-processed kinematic (PPK) positioning technique, Geodesy and Cartography, 2021, 47(2), 66–70, https://doi.org/10.3846/gac.2021.12269
78. Ciećko A., Bakuła M., Grunwald G., Ćwiklak J. Examination of multi-receiver GPS/EGNOS positioning with kalman filtering and validation based on CORS stations. Sensors. 2020, 20, 2732, https://doi.org/10.3390/s20092732
79. MAGNET Tools Website. Available from: https://www.topconpositioning.com/office-software-and-services/survey-software/magnet-tools, (Accessed: 30.12.2025).
80. Gargula T. GPS vector network adjustment on the projection plane of local coordinate system (in Polish). Infrastruktura i Ekologia Terenów Wiejskich, 2010, 6, 133–144.
81. Kadaj R. Tikhonov's mathematical tricks, Geodeta, 2021, 9, 31–35. (in Polish)
82. Osada E. Geodesy (in Polish). Oficyna Wydawnicza Politechniki Wrocławskiej, 2001, 1–222.